Quarter Wavelength Ceramic Combline Filters

Hui-Wen Yao, *Member, IEEE,* Chi Wang, *Student Member, IEEE,* and Kawthar A. Zaki, *Fellow, IEEE*

***Abstract*— A rigorous method for analysis of coupled dielectric quarter wavelength combline resonators is presented. The resonant frequencies and coupling coefficients of the resonators coupled by different coupling structures are investigated. A filter design technique based on the results of numerical analysis is described. A slot coupled filter and a monoblock elliptic function filter are designed. Excellent experimental results verify the theory.**

I. Introduction

THE RAPID EXPANSION of mobile communication market demands a huge amount of compact and inexpensive hand-held communication sets. Reducing filter's size and cost are very important for a high quality and low cost hand-held set. One of the most suitable ways of miniaturizing the filters and reducing the cost is to use high dielectric constant and low loss ceramic material in quarter wavelength combline type filters [1]–[4].

An inhomogeneous dielectric block combline filter was first introduced in [1], where quarter wavelength dielectric combline resonant blocks are coupled by unplated full-through air grooves. A similar inhomogeneous dielectric monoblock filter, using full-through air holes to provide the required interresonator couplings, is presented in [3]. In both cases, the couplings between adjacent resonators are computed using the finite difference method by treating the coupled resonators as coupled parallel TEM transmission lines. This treatment is valid only when the air grooves extend through the dielectric and the operating frequency is well below the cut-off frequencies of all higher order modes of the coupled lines. Another drawback of the method is the difficulty of obtaining convergent results when the dimensions of air grooves are very small [1]. In addition to the full-through air grooves, irises between resonators are also employed in construction of quarter wavelength combline filters in [4], where the iris dimensions are determined experimentally.

To make accurate and efficient designs of high performance quarter wavelength dielectric combline filters, investigation of new coupling structures and precise computation of the coupling coefficients are desired. In this paper, a full wave method [6] is applied to analyze the resonant performance of a dielectric combline cavity perturbed by a partial height air groove and to compute the couplings between two quarter wavelength resonators coupled by different coupling structures such as partial or full height air grooves, air holes, and coupling irises. Design of quarter wavelength combline filters is carried out and constructed. Expermental results verify the validation and accuracy of the method.

Manuscript received March 29, 1996.

H.-W. Yao is with CTA Incorporated, Rockville, MD 20852 USA.

C. Wang and K. A. Zaki are with the Department of Electrical Engineering, University of Maryland, College Park, MD 20742 USA.

Publisher Item Identifier S 0018-9480(96)08545-6.

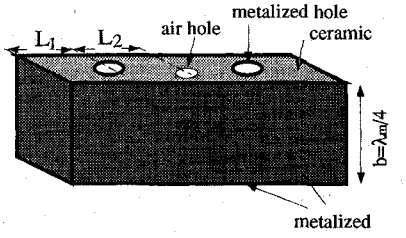

Fig. 1. Schematic structure of two dielectric quarter wavelength combline resonators coupled by a partial height air hole.

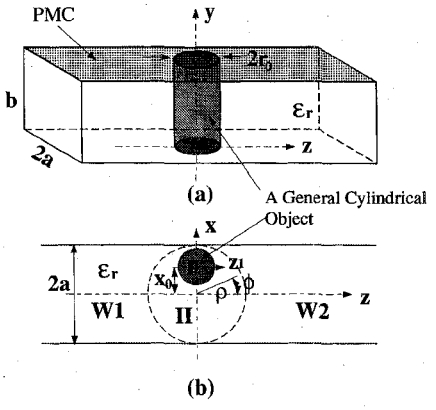

Fig. 2. Configuration of a general off-center cylindrical object in a rectangular waveguide.

II. Analysis

A schematic structure of two dielectric combline resonators coupled by a partial height off-center air hole is shown in Fig. 1. The air hole could be replaced by an air gap, a slot, or other coupling structure. Since the dielectric constant of the material usually is high ($\epsilon_r > 20$), the electromagnetic fields are trapped inside the material and the unmetalized top surface of the structure can be viewed as a perfect magnetic conducting (PMC) surface when dealing with the numerical solution. Without the coupling structure, the resonators will resonate at quarter wavelength and there will be no coupling between resonators due to the electric-magnetic phase cancellation of quarter wavelength coupled lines [5].

The key of solving the problem is to acquire the generalized scattering matrix of a general off-center cylindrical object in a rectangular waveguide with the top surface of PMC as shown in Fig. 2. In this paper, the general cylindrical object could be either a full-through metal post representing the resonator or an air hole representing the coupling structure.

0018–9480/96$05.00 © 1996 IEEE

Similar to [6], the structure is divided into a cylindrical interaction region ($\rho \le a$) and two waveguide region W_1 and W_2 by introducing an artificial cylindrical boundary at $\rho = a$. The cylindrical region could be viewed as a cylindrical object in a radial waveguide where the cylindrical object is not concentric with the main waveguide. Two coordinate systems (ρ, ϕ, y) and (ρ_1, ϕ_1, y) can be established in terms of the center of the main waveguide and the center of the cylindrical object, respectively. The eigenmodes in each coordinate system are TE_y (h) modes and TM_y (e) modes, where the eigenfields can be solved in terms of the y-components of the H-field and E-field, respectively. A complete set of the eigenmodes, which is necessary for solving the asymmetric problem shown in Fig. 2, should include the two orthogonal solutions—$\sin(\phi)$ dependent solutions $(p = s)$ and $\cos(\phi)$ dependent solutions $(p = c)$.

The y-component field of two orthogonal TE_y modes can be solved as

$$j\omega\mu H^{ph}_{ynm}(\rho,\phi,y) = Z_n(\xi^h_m\rho)\Phi^{ph}_n(\phi)h_{ym}(k^h_m,y) \quad p = s,c \tag{1a}$$

with

$$\Phi^{ph}_n(\phi) = \begin{cases} \cos(n\phi) & n = 0,1,2,\cdots \quad \text{if } p = c \\ -\sin(n\phi) & n = 1,2,\cdots \quad \text{if } p = s \end{cases} \tag{1b}$$

where $h_{ym}(k^h_m, y)$ and k^h_m are y-dependent eigenfield and wave number; $\xi^{h^2}_m = k_0^2\epsilon_r - k^{h^2}_m$; $Z_n(\xi_m\rho)$ represents $J_n(\xi_m\rho)$ or $Y_n(\xi_m\rho)$—the first kind or the second kind of Bessel functions if $\xi^2_m \ge 0$ and $I_n(|\xi_m|\rho)$ or $K_n(|\xi_m|\rho)$—the first kind or the second kind of modified Bessel functions if $\xi^2_m < 0$, respectively.

The y-component field of TM_y mode can be expressed as

$$E^{pe}_{ynm}(\rho,\phi,y) = Z_n(\xi^e_m\rho)\Phi^{pe}_n(\phi)e_{ym}(k^e_m,y) \quad p = s,c \tag{2a}$$

where

$$\Phi^{pe}_n(\phi) = \begin{cases} \sin(n\phi) & n = 1,2,\cdots \quad \text{if } p = s \\ \cos(n\phi) & n = 0,1,2,\cdots \quad \text{if } p = c \end{cases} \tag{2b}$$

where $e_{ym}(k^e_m, y)$ and k^e_m are y-dependent eigenfield and wave number; $\xi^{e^2}_m = k_0^2\epsilon_r - k^{e^2}_m$.

$h_{ym}(k^h_m, y)$ and $e_{ym}(k^e_m, y)$ are determined only by the structure in y-direction which can be generally considered as a multilayer parallel plane bounded in y-direction. For one-layer (uniform) and two-layer parallel planes with PMC at its top and PEC (perfect electrical conductor) at its bottom, the solutions are given in the Appendix.

The total fields in the cylindrical region can be expressed as a superposition of the complete set of the eigenmodes including the out-going waves (J_n or I_n dependent waves) and inner-going waves (Y_n or K_n dependent waves) similar to (1) in [6].

Enforcing the boundary conditions at boundary $\rho_1 = r_0$ yields the following equations

$$\{\vec{E}^{\mathrm{II}}_t(\rho_1,\phi_1,y) - \vec{E}^{\mathrm{I}}_t(\rho_1,\phi_1,y)\}_{\rho_1=r_0} = 0 \tag{3a}$$

$$\{\vec{H}^{\mathrm{II}}_t(\rho_1,\phi_1,y) - \vec{H}^{\mathrm{I}}_t(\rho_1,\phi_1,y)\}_{\rho_1=r_0} = 0 \tag{3b}$$

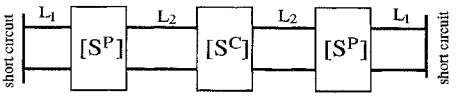

Fig. 3. S-matrix network representation of the coupled structure.

where the subscript 't' represents the transverse fields with respect to the y-direction; the superscript 'I' and 'II' represent region I and region II as shown in Fig. 2. When region I is a perfect conductor, the fields in the region will be all zeros.

Taking the cross inner products to the above equations and applying the mode orthogonality among the modes with different ρ variations, one may obtain

$$[[M^{\mathrm{II}}_C]_{n'}\ [M^{\mathrm{II}}_D]_{n'}]\begin{bmatrix} \boldsymbol{C}^{\mathrm{II}}_{\boldsymbol{n'}} \\ \boldsymbol{D}^{\mathrm{II}}_{\boldsymbol{n'}} \end{bmatrix} = 0 \qquad n' = 0,1,2,\cdots N_\phi \tag{4a}$$

with

$$\boldsymbol{C}'^{\mathrm{II}}_{\boldsymbol{n'}} = \{C'^{\mathrm{II}pq}_{n'm}; m = 1,\cdots,N_y; \quad p = s,c; \quad q = h,e\}^T \tag{4b}$$

$$\boldsymbol{D}'^{\mathrm{II}}_{\boldsymbol{n'}} = \{D'^{\mathrm{II}pq}_{n'm}; m = 1,\cdots,N_y; \quad p = s,c; \quad q = h,e\}^T \tag{4c}$$

where N_ϕ and N_y are the maximum mode index in ϕ and y directions, respectively $C'^{\mathrm{II}pq}_{n'm}$ and $D'^{\mathrm{II}pq}_{n'm}$ are field coefficients of a given eigenmode related to the outer-going waves and inner-going waves in region II in terms of the local coordinate system (ρ_1, ϕ_1, y), respectively, $[M^{\mathrm{II}}_C]_{n'}$ and $[M^{\mathrm{II}}_D]_{n'}$ are matrices determined by the self inner products and the mutual inner products.

The set of matrix equations may be further expressed in a new matrix form as

$$[[M^{\mathrm{II}}_C][M^{\mathrm{II}}_D]]\begin{bmatrix} \boldsymbol{C}'^{\mathrm{II}} \\ \boldsymbol{D}'^{\mathrm{II}} \end{bmatrix} = 0 \tag{5a}$$

with

$$[M^{\mathrm{II}}_L] = \begin{bmatrix} [M^{\mathrm{II}}_L]_0 & & & \\ & [M^{\mathrm{II}}_L]_1 & & 0 \\ & & \ddots & \\ & 0 & & [M^{\mathrm{II}}_L]_{N_\phi} \end{bmatrix} \qquad L = C, D \tag{5b}$$

$$\boldsymbol{C}'^{\mathrm{II}} = \begin{bmatrix} \boldsymbol{C}'^{\mathrm{II}}_{\boldsymbol{0}} \\ \boldsymbol{C}'^{\mathrm{II}}_{\boldsymbol{1}} \\ \vdots \\ \boldsymbol{C}'^{\mathrm{II}}_{\boldsymbol{N_\phi}} \end{bmatrix}; \qquad \boldsymbol{D}'^{\mathrm{II}} = \begin{bmatrix} \boldsymbol{D}'^{\mathrm{II}}_{\boldsymbol{0}} \\ \boldsymbol{D}'^{\mathrm{II}}_{\boldsymbol{1}} \\ \vdots \\ \boldsymbol{D}'^{\mathrm{II}}_{\boldsymbol{N_\phi}} \end{bmatrix}. \tag{5c}$$

From the uniqueness of the solutions of Maxwell's equations, the fields at the points outside the region of the cylindrical object can be expanded by the eigenmodes in either (ρ, ϕ, y) or (ρ_1, ϕ_1, y) without changing the properities of the fields. Using this fact in conjunction with the addition theorems for Bessel functions [7] [8], the following eigenfield transformations for TE_y modes and TM_y modes between the two parallel shifted cylindrical coordinate systems can be

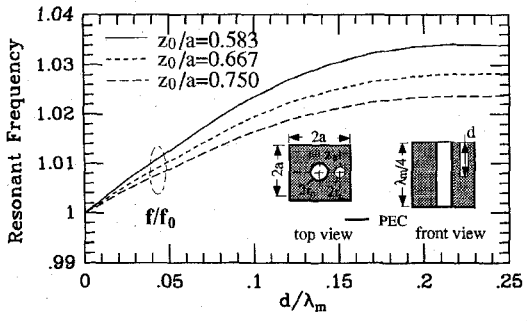

Fig. 4. Normalized resonant frequency of a quarter wavelength combline cavity tuned by a partial height air hole. $2a/\lambda_m = 0.0578$, $r_0/a = 0.275$, $r_h/a = 0.2$, $\epsilon_r = 38.6$, and $f_0 = 0.915$ GHz.

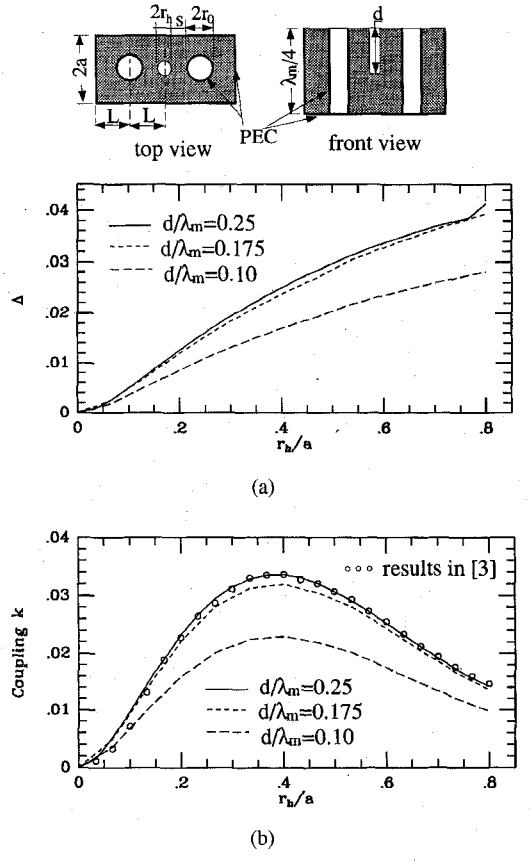

Fig. 5. (a) Frequency shift and (b) coupling coefficients of quarter wavelength rods coupled by partial length air holes. $2a/\lambda_m = 0.1432$, $r_0/a = 0.4$, $s/a = 0.2667$, $L = r_0 + r_h + s$, $\epsilon_r = 80$, and $f_0 = 0.8$ GHz.

derived as

$$\begin{bmatrix} \boldsymbol{b_m^{ch}} \\ \boldsymbol{-b_m^{sh}} \end{bmatrix} = \begin{bmatrix} [F_{cc}^h] & [F_{cs}^h] \\ [F_{sc}^h] & [F_{ss}^h] \end{bmatrix} \begin{bmatrix} \boldsymbol{b_m'^{ch}} \\ \boldsymbol{-b_m'^{sh}} \end{bmatrix} = [F^h] \begin{bmatrix} \boldsymbol{b_m'^{ch}} \\ \boldsymbol{-b_m'^{sh}} \end{bmatrix} \quad \text{for TE}_y \text{ modes} \tag{6a}$$

$$\begin{bmatrix} \boldsymbol{b_m^{ce}} \\ \boldsymbol{b_m^{se}} \end{bmatrix} = \begin{bmatrix} [F_{cc}^e] & [F_{cs}^e] \\ [F_{sc}^e] & [F_{ss}^e] \end{bmatrix} \begin{bmatrix} \boldsymbol{b_m'^{ce}} \\ \boldsymbol{b_m'^{se}} \end{bmatrix} = [F^e] \begin{bmatrix} \boldsymbol{b_m'^{ce}} \\ \boldsymbol{b_m'^{se}} \end{bmatrix} \quad \text{for TM}_y \text{ modes} \tag{6b}$$

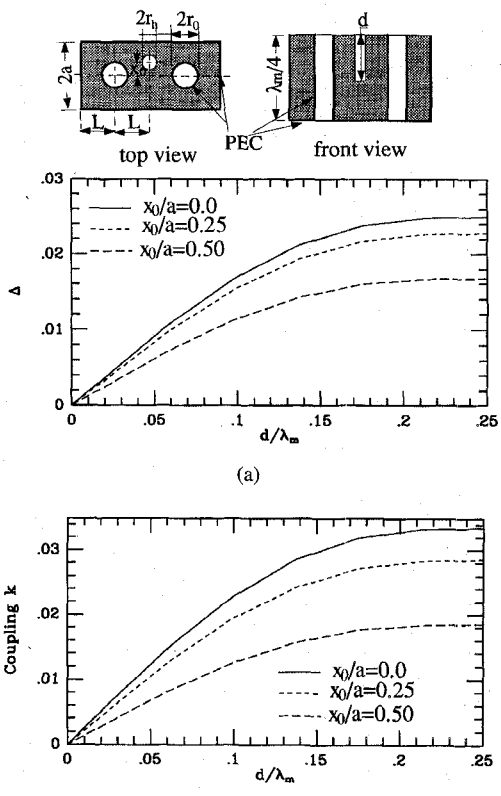

Fig. 6. (a) Frequency shift and (b) coupling coefficients of quarter wavelength rods coupled by partial length off-center air holes. $2a/\lambda_m = 0.1432, r_0/a = r_h/a = 0.4$, $L/a = 1.0667, \epsilon_r = 80$, and $f_0 = 0.8$ GHz.

where

$$\boldsymbol{a_m^{sq}} = \begin{bmatrix} a_{1m}^{sq} \\ a_{2m}^{sq} \\ \vdots \\ a_{N_\phi m}^{sq} \end{bmatrix}; \quad \boldsymbol{a_m^{cq}} = \begin{bmatrix} a_{0m}^{cq} \\ a_{1m}^{cq} \\ \vdots \\ a_{N_\phi m}^{cq} \end{bmatrix}$$
$$\boldsymbol{a} = \boldsymbol{b}, \boldsymbol{b'}; \quad q = h, e \tag{6c}$$

b_{nm}^{pq} and $b_{n'm}^{pq}$ could be C_{nm}^{pq} and $C_{n'm}^{\prime pq}$ or D_{nm}^{pq} and $D_{n'm}^{\prime pq}$, respectively, where C_{nm}^{pq} and D_{nm}^{pq} are field coefficients of the eigenmode in coordinate system (ρ, ϕ, y) and $C_{n'm}^{\prime pq}$ and $D_{n'm}^{\prime pq}$ are field coefficients of the eigenmode in coordinate system (ρ_1, ϕ_1, y).

The elements of the matrices are given by

$$\begin{aligned}
(F_{cc}^q)_{0n'} &= \delta_{n'} \Delta_{n'} \wp_{n'}(\xi_m^q \rho_0) \cos n' \phi_0 \\
(F_{cc}^q)_{nn'} &= \delta_{n-n'} [\wp_{n-n'}(\xi_m^q \rho_0) \cos(n-n')\phi_0 \\
&\quad + \Delta_{n'} \wp_{n+n'}(\xi_m^q \rho_0) \cos(n+n')\phi_0] \\
(F_{cs}^q)_{0n'} &= \delta_{n'} \Delta_{n'} \wp_{n'}(\xi_m^q \rho_0) \sin n' \phi_0 \\
(F_{cs}^q)_{nn'} &= \delta_{n-n'} [-\wp_{n-n'}(\xi_m^q \rho_0) \sin(n-n')\phi_0 \\
&\quad + \Delta_{n'} \wp_{n+n'}(\xi_m^q \rho_0) \sin(n+n')\phi_0] \\
(F_{sc}^q)_{nn'} &= \delta_{n-n'} [\wp_{n-n'}(\xi_m^q \rho_0) \sin(n-n')\phi_0 \\
&\quad + \Delta_{n'} \wp_{n+n'}(\xi_m^q \rho_0) \sin(n+n')\phi_0] \\
(F_{ss}^q)_{nn'} &= \delta_{n-n'} [\wp_{n-n'}(\xi_m^q \rho_0) \cos(n-n')\phi_0 \\
&\quad - \Delta_{n'} \wp_{n+n'}(\xi_m^q \rho_0) \cos(n+n')\phi_0]
\end{aligned} \tag{7a}$$

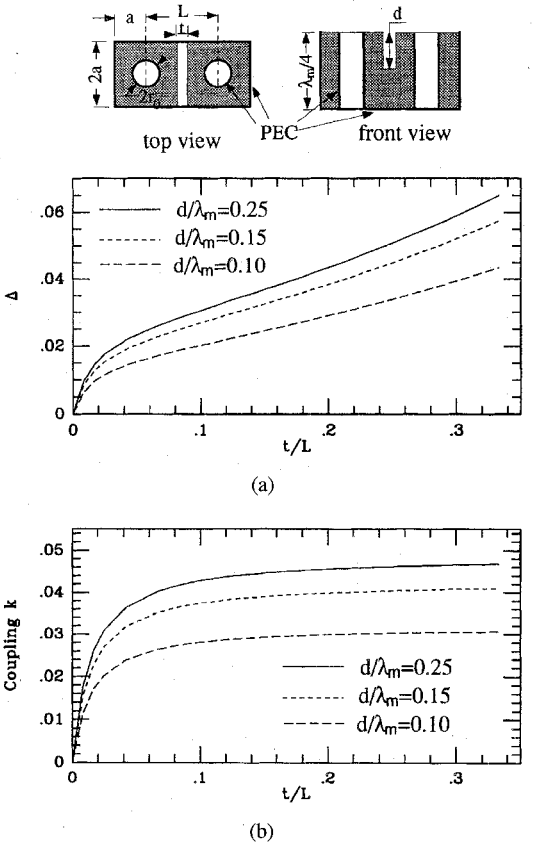

Fig. 7. (a) Frequency shift and (b) coupling coefficients of quarter wavelength rods coupled by partial length air gaps. $2a/\lambda_m = 0.0578, r_0/a = 0.275, L = 2a, \epsilon_r = 38.6$, and $f_0 = 0.915$ GHz.

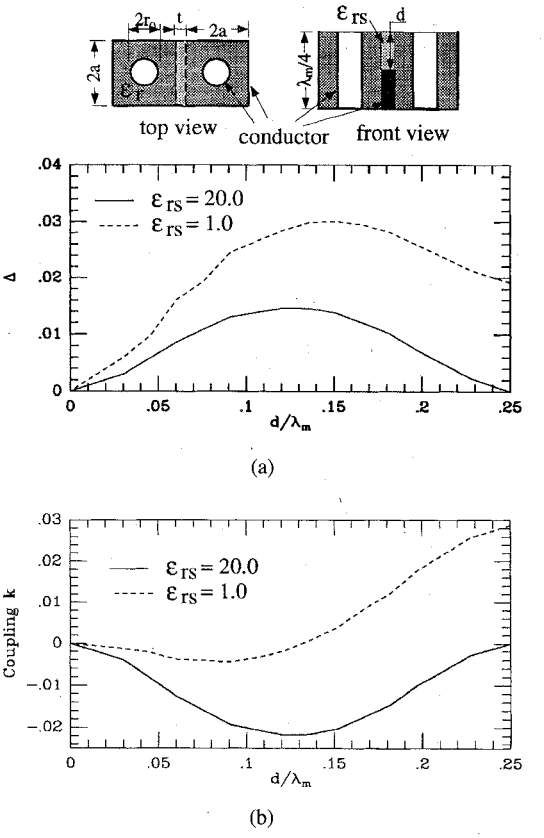

Fig. 8. (a) Frequency shift and (b) coupling coefficients of quarter wavelength rods coupled by air filled and dielectric filled slots. $2a/\lambda_m = 0.1432, r_0/a = 0.3333, t/a = 0.127, \epsilon_r = 20$, and $f_0 = 0.8$ GHz.

where

$$\wp_n(\xi_m^q \rho_0) = \begin{cases} J_n(\xi_m^q \rho_0) & \text{if } Z_{n'} \in \{J_{n'}, Y_{n'}\} \\ I_n(|\xi_m^q|\rho_0) & \text{if } Z_{n'} \in \{I_{n'}, K_{n'}\} \end{cases} \tag{7b}$$

$$\delta_n = \begin{cases} 1 & \text{if } Z_{n'} \in \{J_{n'}, Y_{n'}, K_{n'}\} \\ (-1)^n & \text{if } Z_{n'} = I_{n'} \end{cases} \tag{7c}$$

$$\Delta_{n'} = \begin{cases} (-1)^{n'} & \text{if } Z_{n'} \in \{J_{n'}, Y_{n'}\} \\ 1 & \text{if } Z_{n'} \in \{I_{n'}, K_{n'}\} \end{cases} \tag{7d}$$

For the configuration shown in Fig. 2, $\rho_0 = x_0$ and $\phi_0 = \pi/2$.

By using (5) and (6), the scattering from the off-center cylindrical object in the coordinate system (ρ, ϕ, y) can be acquired as

$$[[M_C^{\mathrm{II}}][M_D^{\mathrm{II}}]][T_R]\begin{bmatrix} \boldsymbol{C}^{\mathrm{II}} \\ \boldsymbol{D}^{\mathrm{II}} \end{bmatrix} = 0 \tag{8}$$

where $\boldsymbol{C}^{\mathrm{II}}$ and $\boldsymbol{D}^{\mathrm{II}}$ are field coefficient vectors of all the eigenmodes in region II in terms of coordinate system (ρ, ϕ, y). The elements of the transformation matrix $[T_R]$ are either the elements of $[F^e]^{-1}$ and $[F^h]^{-1}$ or zeros depending on the mode arrangement. Obviously, $[T_R]$ will be an identity matrix if two coordinate systems are concentric.

Following the same procedure in [6], the generalized S-matrix $[S^P]$ of the metal post and $[S^C]$ of the air hole

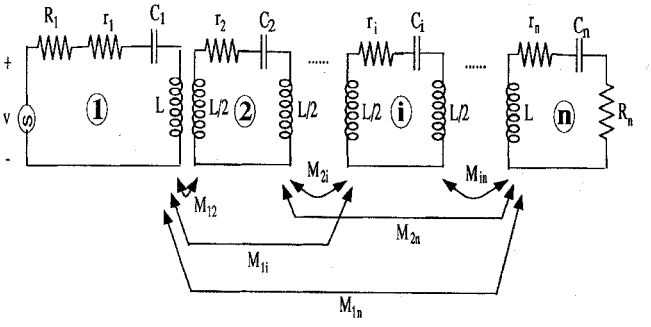

Fig. 9. An equivalent circuit of a general bandpass filter.

can be obtained by enforcing the boundary conditions on the artificial cylindrical boundary $\rho = a$ and applying (8). The solution exhibits the same convergence as presented in [6].

If the coupling structure is a partial height air gap or a slot instead of an air hole, its generalized S-matrix $[S^C]$ can also be readily solved by conventional mode matching method.

With the knowledge of generalized scattering matrices of all the discontinuities involved in the coupled structure, the eigen equations for the natural resonant frequencies can be derived from Fig. 3 by applying the cascading procedure using S-matrices [9] in conjunction with the termination conditions. Two natural resonant frequencies f_e and f_m, corresponding to PEC and PMC at the symmetrical plane of the structure, can

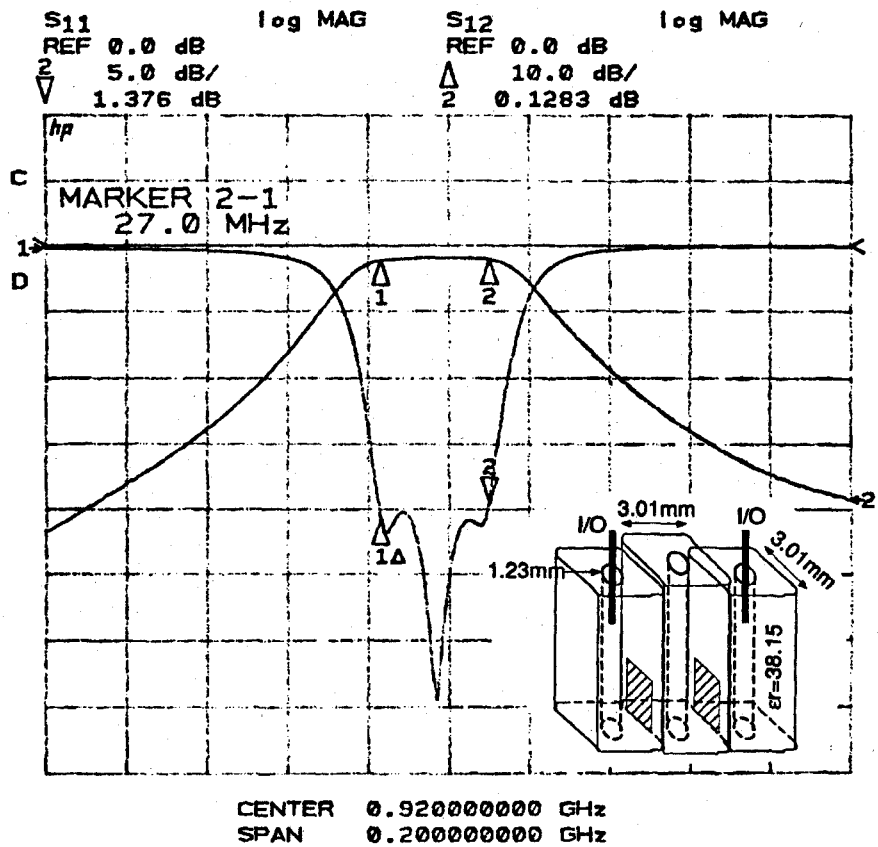

Fig. 10. Measured responses of three-pole slot coupled quarter wavelength dielectric combline filter.

be acquired from the equations, and the coupling coefficient can be computed as [10]

$$k = \frac{f_e^2 - f_m^2}{f_e^2 + f_m^2} \tag{9}$$

$k > 0$ represents that the coupling is mainly contributed by the magnetic fields; $k < 0$ indicates that the electric field coupling is dominant.

The frequency shift due to the loading of coupling may be defined as

$$\Delta = \frac{f_r - f_0}{f_0} \tag{10}$$

where f_0 is the resonant frequency of the quarter wavelength resonator without the loading effect; $f_r = 0.5(f_e + f_m)$ is the midfrequency of the coupled resonators.

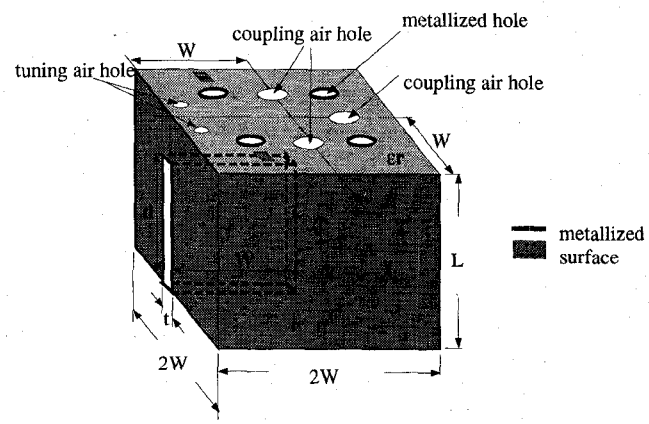

Fig. 11. Configuration of a monoblock 4-pole elliptic function filter.

III. Results

A. Resonant Frequency and Coupling

A dielectric combline cavity usually resonates at the frequency of a quarter wavelength. The resonant frequency could be tuned by making an air hole in the cavity. Fig. 4 shows the tunability using air holes with different heights and locations. In general, an air hole shifts the resonant frequency higher. The closer the air hole to the resonant rod, the larger the frequency shift.

Fig. 5 presents the midfrequency shift and the couplings of two quarter wavelength rods coupled by partial height air holes varying the radii, where λ_m is the wavelength in the medium at frequency f_0. Also presented in the figure are the couplings of full through air hole ($d/\lambda_m = 0.25$) computed by the finite difference method in [3]. Fig. 6 shows the results of two resonators coupled by a partial height off-center air hole. As expected, the coupling decreases with the increase of the off-set of the coupling hole. Fig. 7 gives the results of the frequency shift and the coupling coefficients of two coupled resonators by rectangular air gaps with fixed distance between the resonators. As indicated in [2], the figure shows that the couplings increase with increasing the degree of inhomogeneity, i.e., the height and the thickness of the gaps. However, the increase of coupling tends to "saturate" while

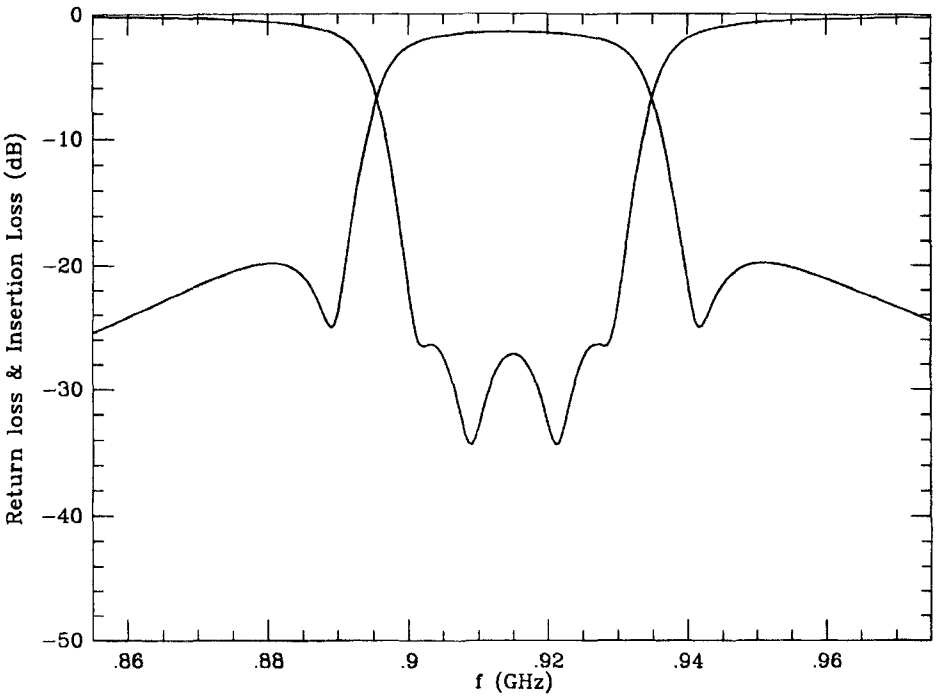

Fig. 12. Ideal response of the 4-pole elliptic function filter.

the midfrequency shift continues to increase. Both air hole and air gap provide only the magnetic (positive) coupling. To realize the electric (negative) coupling as required in design of elliptic function filters, irises have to be used. The results using iris as coupling structure are presented in Fig. 8, where the irises are opened from the unmetalized side of the coupled cavities. As the figure shows, the relative dielectric constant of the material filling in the irises greatly affects the coupling properties.

B. Filter Design

An equivalent circuit of a general bandpass filter is shown in Fig. 9, where M_{ij} is the mutual inductance between resonator i and j which is related to the coupling coefficient k_{ij} by $k_{ij} = M_{ij}/L$. For given specifications of a filter, the required couplings could be obtained by synthesis [11]. The dimensions of coupling structures can be determined by the method presented in the last section according to the desired coupling values. In addition to providing coupling, each coupling structure also contributes loading to each of its coupled cavities. As shown previously, the loading makes each cavity resonate at a higher frequency. In order to have all the cavities resonate at filter's center frequency f_0 when coupled together, each individual cavity has to be designed at a lower frequency to compensate for the loading effect of the couplings. For cavity i, it can be readily proved [4] that the resonant frequency should be designed at

$$f_{0i} \approx f_0 \left(1.0 - \sum_j \Delta_{ij} \right) \qquad i \neq 1 \text{ or } n \tag{11a}$$

$$f_{0i} \approx f_0 \left(1.0 - \Delta_{0i} - \sum_j \Delta_{ij} \right) \qquad i = 1 \text{ or } n \tag{11b}$$

where Δ_{ij} is the frequency shift due to the loading of interresonator coupling and can be calculated by the mode matching method; Δ_{0i} is the contribution of the input/output loading and may be determined experimentally.

As the application of the accurate analysis and design technique, a slot coupled quarter wavelength combline three-pole Tchebyscheff filter with center frequency of 0.915 GHz and bandwidth of 27 MHz is designed and constructed. The measured results without tuning the dimensions of the slots and the length of the middle resonator are presented in Fig. 10 showing excellent response with required center frequency and bandwidth. The average realized un-loaded Q is estimated to be 250. Another example is the design of a monoblock 4-pole elliptic function filter with center frequency of 0.915 GHz and bandwidth of 30 MHz. The configuration of the filter is shown in Fig. 11. The three full through air holes in the figure are used to provide the required magnetic couplings, and the slot is applied to provide the electric coupling. The loading effect of the input/output is compensated experimently by two partial height air holes. The ideal response of the filter is given in Fig. 12.

IV. Conclusions

A full wave method is developed to analyze the resonant and coupling properties of quarter wavelength dielectric combline resonators coupled by different coupling structures. The technique provides an accurate and efficient way for designing low loss and small size combline filters for mobile communication

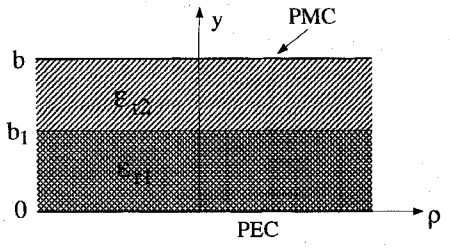

Fig. 13. Configuration of a two-layer parallel plane.

applications. The accuracy and validation of the method are verified by experiments.

APPENDIX

Fig. 13 shows the configuration of a two-layer parallel plane waveguide bounded in y direction with PMC at the top surface. When $\epsilon_{r1} = \epsilon_{r2} = \epsilon_r$, the structure becomes a one-layer parallel plane waveguide. The eigenmodes existing in the structure are:

TE_y^p **mode:**

For one-layer case

$$h_{ym}(k_m^h, y) = \sin(k_m^h y) \tag{A1}$$

$$k_m^h = \frac{(2m-1)\pi}{2b} \qquad m = 1, 2, \cdots \tag{A2}$$

For two-layer case

$$h_{ym}(k_m^h, y) = \begin{cases} \dfrac{\sin(k_m^{(1)h} y)}{\sin(k_m^{(1)h} b_1)} & 0 \le y < b_1 \\ \dfrac{\cos[k_m^{(2)h}(y-b)]}{\cos[k_m^{(2)h}(b_1-b)]} & b_1 \le y < b \end{cases} \tag{A3}$$

with the characteristic equation

$$k_m^{(1)h} \cot(k_m^{(1)h} b_1) = -k_m^{(2)h} \tan[k_m^{(2)h}(b_1 - b)] \tag{A4}$$

$$k_0^2 \epsilon_{r1} - (k_m^{(1)h})^2 = k_0^2 \epsilon_{r2} - (k_m^{(2)h})^2 \tag{A5}$$

TM_y^p **mode:**

For one-layer case

$$e_{ym}(k_m^e, y) = \cos(k_m^e y) \tag{A6}$$

$$k_m^e = \frac{(2m-1)\pi}{2b} \qquad m = 1, 2, \cdots \tag{A7}$$

For two-layer case

$$e_{ym}(k_m^e, y) = \begin{cases} \dfrac{1}{\epsilon_{r1}} \dfrac{\cos(k_m^{(1)e} y)}{\cos(k_m^{(1)e} b_1)} & 0 \le y < b_1 \\ \dfrac{1}{\epsilon_{r2}} \dfrac{\sin[k_m^{(2)e}(y-b)]}{\sin[k_m^{(2)e}(b_1-b)]} & b_1 \le y < b \end{cases} \tag{A8}$$

with the characteristic equation

$$\frac{1}{\epsilon_{r1}} k_m^{(1)e} \tan(k_m^{(1)e} b_1) = -\frac{1}{\epsilon_{r2}} k_m^{(2)e} \cot[k_m^{(2)e}(b_1 - b)] \tag{A9}$$

$$k_0^2 \epsilon_{r1} - (k_m^{(1)e})^2 = k_0^2 \epsilon_{r2} - (k_m^{(2)e})^2. \tag{A10}$$

REFERENCES

[1] A. Fukasawa, "Analysis and composition of a new microwave filter configuration with inhomogeneous dielectric medium," *IEEE Trans. Microwave Theory Tech.*, vol. MTT-30, pp. 1367–1375, Sept. 1982.

[2] R. Levy, "Simplified analysis of inhomogeneous dielectric block combline filters," in *1990 IEEE MTT-S, Int. Microwave Symp. Dig.*, pp. 135–138.

[3] C.-C. You, C.-L. Huang, and C.-C. Wei, "Single-block ceramic microwave bandpass filters," *Microwave J.*, pp. 24–35, Nov. 1994.

[4] K. Hano, H. Kohriyama, and K.-I. Sawamoto, "A direct-coupled $\lambda/4$-coaxial resonator bandpass filter for land mobile communications," *IEEE Trans. Microwave Theory Tech.*, vol. MTT-34, pp. 972–976, Sept. 1986.

[5] J. T. Bolljahn and G. L. Matthaei, "A study of the phase and filter properties of arrays of parallel conductors between ground planes," *Proc. IRE*, vol. 50, pp. 299–311, 1962.

[6] H.-W. Yao, K. A. Zaki, A. E. Atia, and R. Hershtig, "Full wave modeling of conducting posts in rectangular waveguide and its applications to slot coupled combline filters," *IEEE Trans. Microwave Theory Tech.*, vol. 43, pp. 2824–2830, Dec. 1995.

[7] R. Gesche, "Transformation of the wave equation solution between parallel displaced cylindrical coordinate systems," *Arch. Elektrotech.*, vol. 67, pp. 391–394, 1984.

[8] R. Gesche and N. Löchel, "Scattering by a lossy dielectric cylinder in a rectangular waveguide," *IEEE Trans. Microwave Theory Tech.*, vol. 36, pp. 137–144, Jan. 1988.

[9] J. Pace and R. Mittra, "Generalized scattering matrix analysis of waveguide discontinuity problems," in *Quasi-Optics XIV*. New York: Polytech. Inst. Brooklyn Press, 1964, pp. 172–194.

[10] H.-W. Yao, J.-F. Liang, and K. A. Zaki, "Accuracy of coupling computations and its application to DR filter design," *1994 IEEE MTT-S Int. Microwave Symp. Dig.*, pp. 723–726.

[11] A. E. Atia and A. E. Williams, "Narrow-bandpass waveguide filters," *IEEE Trans. Microwave Theory Tech.*, vol. MTT-20, pp. 258–265, Apr. 1972.

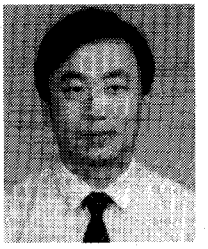

Hui-Wen Yao (S'92–M'95) received the B.S. and M.S. degrees from Beijing Institute of Technology, Beijing, China, in 1983 and 1986, respectively, and Ph.D. degree from University of Maryland, College Park, in 1995, all in electrical engineering.

From 1986 to 1991, he was a Lecturer with the Department of Electrical Engineering, Beijing Institute of Technology, where his research dealt mainly with EM radiation, scattering, and antenna design. From 1991 to 1992, he held the position of Teaching Assistant with the Electrical Engineering Department, Wright State University, Dayton, OH, where he worked on microstrip circuits and transient scattering by cylinders. From 1992 to 1995, he was a research assistant in the Microwave Laboratory, Department of Electrical Engineering, University of Maryland, College Park, where he worked on analysis, modeling and design of microwave and millimeter-wave devices and circuits. He is now with CTA Incorporated, Rockville, MD, working on satellite communications.

Chi Wang (S'96), for a photograph and biography, see this issue, p. 2542.

Kawthar A. Zaki (SM'85–F'91), for a photograph and biography, see this issue, p. 2542.